Numerical analysis of water flow in a centrifugal pump for Diesel engine cooling system.

Rodrigo Lima Kagami, rkagami@ita.br
Edson Luiz Zaparoli, zaparoli@ita.br
Cláudia Regina de Andrade, claudia@ita.br
Instituto Tecnológico de Aeronáutica, Divisão Engenharia Mecânica, Praça Marechal Eduardo Gomes, 50, Vila das Acácias, CEP 12288-900, São José dos Campos, SP

Fabio Yukio Kurokawa, fabio.kurokawa@navistar.com.br
Navistar South America, MWM International Motores, Avenida Nações Unidas, 22.002, CEP 04795-915, São Paulo, SP

Abstract.
The water flow in a centrifugal pump for Diesel engine cooling system was numerically simulated employing finite volume method to solve the modelling equations (mass, momentum and turbulence model) in a rotating reference frame approach. The pump moving parts render the problem unsteady when viewed from a stationary reference system. However, using a rotating reference frame, the flow through the moving parts can be modeled as a steady-state problem with respect to the moving system. The discretized equations system for pressure and velocity components was iteratively solved using a pressure based formulation (SIMPLE segregated algorithm). Numerical results obtained using Fluent code showed good agreement with water flow velocities and centrifugal pump performance when compared with experimental measurements. After numerical solution validation, CFD post-processing tools were used to evaluate both rotor and volute internal water flow intending the centrifugal pump performance improvement.

Keywords: water pump, Computational Fluid Dynamics, diesel cooling system

1. INTRODUCTION

The objective of internal combustion engine is to convert chemical energy into mechanical energy and a great amount of this energy is transformed in heat that must be controlled through a cooling system.

The cooling system has two main objectives, firstly warm up the engine and maintains a constant operating temperature. The second objective is to prevent overheating. Formerly, the air cooling system was predominant, nowadays liquid phase cooling systems are much more common. In this case, a centrifugal pump promotes the driving force for the fluid flow through the engine. Centrifugal pumps are employed since they can work with a wide range of working fluids at temperature and pressure levels relatively high (Spence, 2009).

The centrifugal pumps have been experimentally studied by several authors correlating geometry changes to the pressure and velocities variations at the pump. Uchida et al (1971) investigated radial forces and performance of different volute passages and shapes for a one inlet and outlet pump with a direct monitoring of the pressure and changes in axial and radial thrust. A non-intrusive method such as laser velocimetry was used by Visser (1995) to obtain velocity data.

Nowadays, however, the Computational Fluid Dynamics (CFD) became a suitable tool to analyze design and performance improvement of turbomachinery. A good feature of CFD simulations is that estimated results are available in all time and space inside the domain. Furthermore, the progress of CFD technology allows improvement predictions for each specific application. In the 2000s decade, an Euler's solver was the most advanced method available for the solution of impeller-volute interaction in a centrifugal compressor (Hangelstein, 2000). Today, Navier-Stokes commercial solvers have been utilized.

Since the flow through a turbomachinery is turbulent, it is necessary an adequate turbulence model to capture eddy viscosity effects. In industrial problems simulation, is common the use of Reynolds Averaged Navier-Stokes turbulence model (RANS). This approach is sufficient when the concern is mean flow characteristics. In general, a good agreement with experimental results can be obtained employing classical RANS approach (Lucius, 2010).

The herein work focuses on a numerical modeling of a centrifugal pump intending its performance evaluation employing Fluent CFD code. The mathematical model for a moving reference frame is solved utilizing a finite volume method and the turbulent effects are taken account using a two-equations realizable k-ε turbulence model. The validation is performed by comparing numerical solution with experimental data reported by Ojeda (1995). As this validation work shows that the numerical procedure is adequate, the present CFD tool will be utilized to simulate a diesel engine cooling system.

2. 3D SIMULATION OF CENTRIFUGAL PUMP FLOW

A CFD simulation of the flow through the impeller-volute ensemble of a centrifugal pump is accomplished considering incompressible, no-cavitating flow. The pump used for the study is reported in Hamkins and Flack (1987), Miner et al. (1989) and Ojeda et al. (1992). The Figure 1 shows the geometry of the impeller and pump housing.
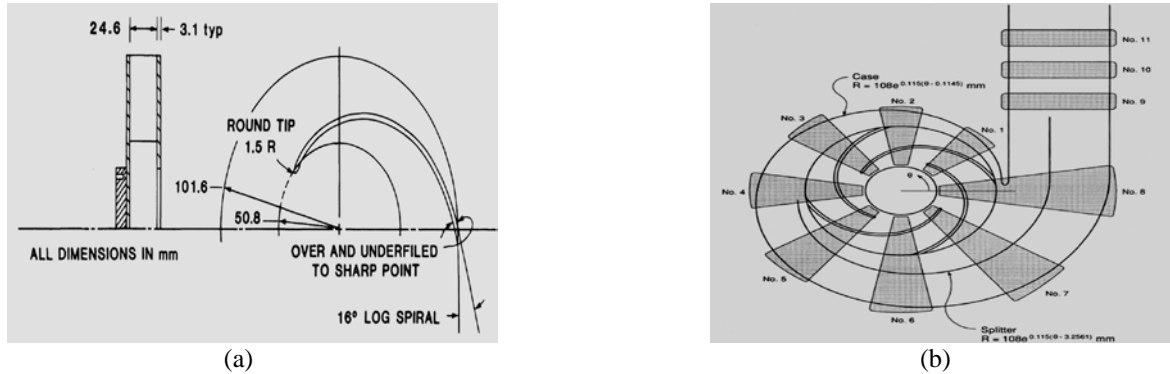

(a)   (b)

Figure 1. (a) Impeller geometry; (b) Volute geometry (Ojeda,1995).

The blades of the impeller and the pump housing are keyed logarithmic spirals formats with 16° e 83°, respectively. The width of the impeller passages is 24.6 mm with a peripheral diameter of 203.2 mm (Figure 1). The impeller is modeled utilizing a moving reference frame model (MRF), with a constant rotational speed, while the inlet duct and the volute are assumed stationary.

2.1. Mathematical Formulation

In a centrifugal pump study, moving parts create transient problems when a stationary reference frame is employed. However, the use of a moving (rotating) reference frame allows the flow around the moving blade can be modeled assuming steady-state flow. This technique can solve typical problems involving moving parts, such as rotating blades and impellers, when the flow of interest is around the moving part. The velocities of the fluid flow can be transformed from a stationary reference frame for a rotating reference frame using the following relationship

$$v_r = v - u_r \tag{1}$$

where

$$u_r = \omega \times r \tag{2}$$

In the above expression v_r is the relative velocity (view from a rotating frame), v is the absolute velocity (view from a stationary frame) and u_r is the whirl speed (velocity due the rotation).

Expressing the conservation and transport equations utilizing the relative velocity as dependent variable, the governing equations of the flow can be expressed as follows:

Mass conservation:
$$\frac{\partial \rho}{\partial t} + \nabla \cdot (\rho v_r) = 0 \tag{3}$$

Momentum:
$$\frac{\partial (\rho v_r)}{\partial t} + \nabla \cdot (\rho v_r v_r) + \rho(2\omega \times v_r + \omega \times \omega \times r) = -\nabla p + \nabla \cdot \overrightarrow{\tau_r} \tag{4}$$

The momentum equations presents two additional acceleration terms: Coriolis acceleration ($2\omega \times v_r$) and the centrifugal acceleration ($\omega \times \omega \times r$). The viscous stress term ($\overrightarrow{\tau_r}$) is identical to the stress tensor for a inertial frame, except that the relative velocity is derived, resulting in

$$\overrightarrow{\tau_r} = \mu_{eff} \left[(\nabla v_r + (\nabla v_r)^{\text{ tr}}) - \frac{2}{3} (\nabla \cdot v_r) I \right] \tag{5}$$

Where μ_{eff} is the effective viscosity (laminar+turbulent viscosity), tr indicates transposed, I is the unitary tensor and the second term in the right side represents the volumetric dilatation effect.

2.2. Turbulence model

Turbulent flows are characterized for fluctuations in the velocity field. These fluctuations may transport quantities such as momentum, energy and species concentration and these transported quantities fluctuate too. Because they are small-scale and high-frequency, fluctuations are computationally expensive for a direct simulation. An alternative to reduce computational effort is decompose the instantaneous Navier-Stokes equations in mean components of flow and fluctuant components, this approach is known as Reynolds averaged Navier-Stokes (RANS). There is no global turbulence model adequate for any kind of case and your choice depends on the physics governing the flow, practices established for a specific problem, level of accuracy required, computational resources available and time available for simulation.

At the present work, the effects of turbulence are calculated using a realizable k-ε model in conjunction with Boussinesq hypothesis. Employing indicial notation, the turbulence stress tensor is evaluated as:

$$-\rho \overline{u_i' u_j'} = \mu_t \left(\frac{\partial u_i}{\partial x_j} + \frac{\partial u_j}{\partial x_i} \right) - \frac{2}{3} \left(\rho k + \mu_t \frac{\partial u_k}{\partial x_k} \right) \delta_{ij} \tag{6}$$

where μ_t represents eddy viscosity, u_i and u_j are the v_r velocity components.

For the realizable k-ε model (Fluent. Inc., 2008), two additional transport equations are solved, the first for turbulent kinetic energy, k, and the second for turbulent dissipation, ε, where the eddy viscosity is calculated as a function of k and ε. The use of this k- ε model is justified by its robustness, economy and relative accuracy for use in engineering practice. The transport equations for k and ε are given by.

$$\frac{\partial (\rho k)}{\partial t} + \frac{\partial (\rho u_i u_j)}{\partial x_j} = \frac{\partial \left[\left(\mu + \frac{\mu_t}{\sigma_k} \right) \frac{\partial k}{\partial x_j} \right]}{\partial x_j} + G_k - \rho \varepsilon \tag{7}$$

$$\frac{\partial (\rho \varepsilon)}{\partial t} + \frac{\partial (\rho \varepsilon u_j)}{\partial x_j} = \frac{\partial \left[\left(\mu + \frac{\mu_t}{\sigma_\varepsilon} \right) \frac{\partial \varepsilon}{\partial x_j} \right]}{\partial x_j} - \rho C_2 \frac{\varepsilon^2}{k + \sqrt{v \varepsilon}} \tag{8}$$

where G_k represents the generation of turbulence kinetic energy due to the mean velocity gradients, μ is the molecular viscosity and v is the kinematic viscosity.

2.3. Boundary conditions

To determine the flow field variables from the governing equations is necessary to specify mathematically the boundary conditions for each dependent variable at the domain boundary, Fluent. Inc. (2008). All these boundary conditions are listed in Tab.1. Mass flow inlet is defined as boundary condition at the domain inlet, providing an inlet uniform mass distribution and allowing the variation of pressure according to the interior domain solution. A static null pressure value is set at domain outlet. All the walls are set as no-slip condition.

Table 1. **Boundary conditions**

Boundary	Boundary condition
Inlet	Mass flow rate; $\frac{\mu_t}{\mu} = 10$; I = 5%
Outlet	Static pressure = 0 Pa
Walls	$v_r = 0$; non-equilibrium wall function

where I is the turbulence intensity level (Fluent. Inc., 2008).

3. Solution Strategy

Numerical simulations of water flow are carried out under standard conditions using Fluent CFD code (Fluent Inc., 2008). The solution technique based on control volume consists in split the computational domain in discrete control volume utilizing a computational mesh and the integration of the governing equations to the individuals control volume to produce algebraic equations for the discrete dependent variables. The linearization of the discrete equations and the

solution of the resultant linear equation set update the dependents variables values. Thus, the non-linear differential partial equation system is solved using a volume finite technique. The velocity field is extracted from the momentum equation while the pressure field is obtained solving the pressure correction equation derived from the manipulation of the continuity equation and momentum equation, utilizing the algorithm SIMPLE. A pressure based solver is also employed. The intake duct is responsible to ensure a fully developed flow at the impeller inlet.

Initially, a triangular mesh was generated employing the Ansys meshing package (Fluent Inc., 2008) and it was converted in a polyhedral mesh using the Fluent inherent capability (available option from mesh menu). Then, a non-structured mesh with polyhedral elements was obtained with 1,372,559 cells. Figure 2 shows the final mesh for the duct-rotor-volute ensemble.
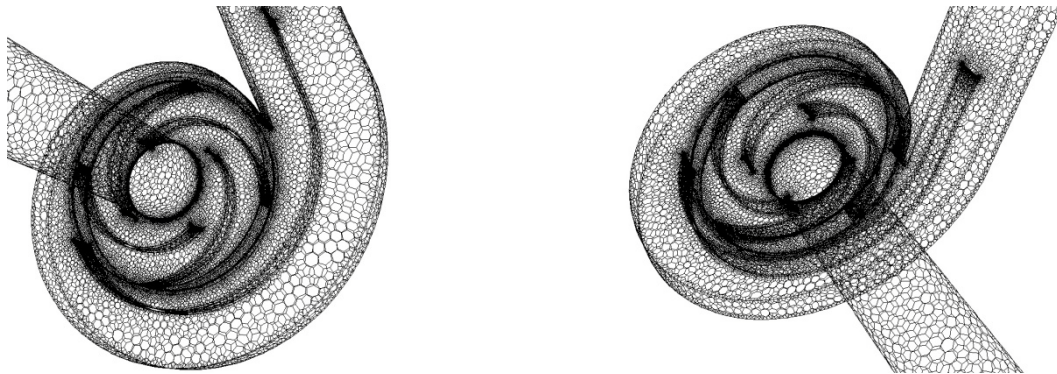
Figure 2. Non-structured polyhedral mesh

In Fig. 3, the mesh generated for the fluid flow domain through the impeller is shown. The refinement mesh is observed at the blades edge. A sensitivity mesh study was performed and the final mesh was chosen by monitoring the convergence of the static pressure integrated at the outlet cross-section area. The adopted mesh (fig 2 and fig 3) represents a trade-off solution between CPU time and convergence study. The MRF approach is utilized for the simulation of the rotational effects at the impeller with a pre-established angular speed of 620 rpm.
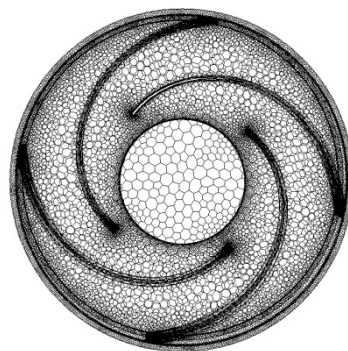
Figure 3. Impeller mesh.

3.1. Comparing numerical results with experimental data

Ojeda et al. (1995) reported pressure measurements around the periphery of the rotor and along the volute wall cover for pumps with a single volute. Figure 4 shows the apparatus utilized to perform the pressure experimental data.
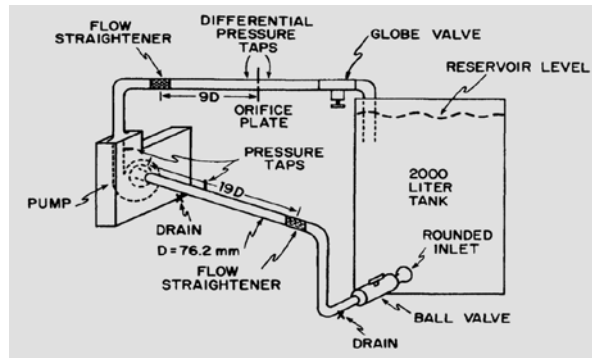
Figure 4. Experimental apparatus (Ojeda,1995).

To compare experimental data and present work results, the rotor domain is modeled utilizing MRF approach with constant rotational speed while the intake duct and volute domains are considered stationary, Fig(5).
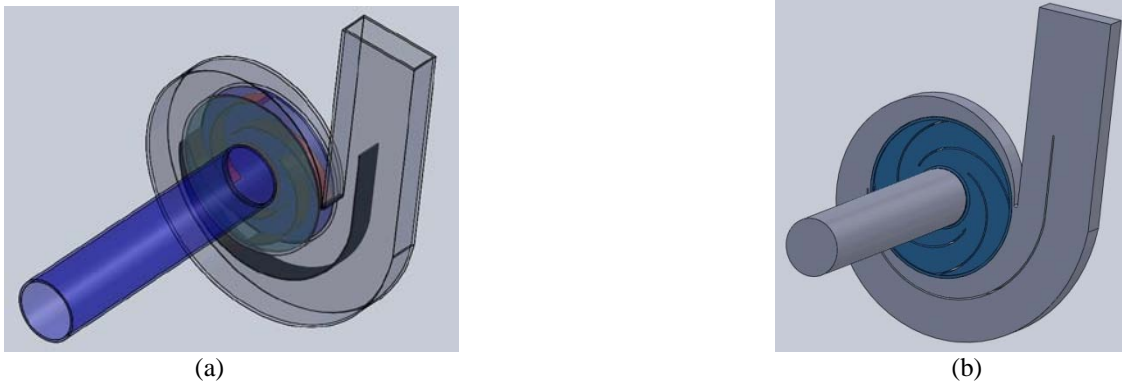

(a)

(b)

Figure 5. (a) CAD model; (b) fluid flow domain.

The total head experimentally measured are compared with numerical results as a function of the volumetric flow through the pump that is calculated as:

$$\dot{Q} = \int_A V_n \, dA \tag{9}$$

$$\bar{H} = \overline{Ptot_o} - \overline{Pstat_i} \tag{10}$$

$$\overline{Ptot_o} = \frac{1}{\dot{m}} \int_A Ptot_o \, d\dot{m} \tag{11}$$

$$\overline{Pstat_i} = \frac{1}{\dot{m}} \int_A Pstat_i \, d\dot{m} \tag{12}$$

where $\dot{m}$ is the mass flow rate, $\bar{H}$ is the total head [Pa]and $\dot{Q}$ is the volumetric flow rate [liters/s], $Ptot_o$ is the outlet total pressure and $Pstat_i$ is the inlet static pressure.

4. RESULTS

In order to validate the CFD model, numerical data are compared with experimental measurements, Fig.6. The design point of the pump is 6.3 l/s according to Ojeda (1995).
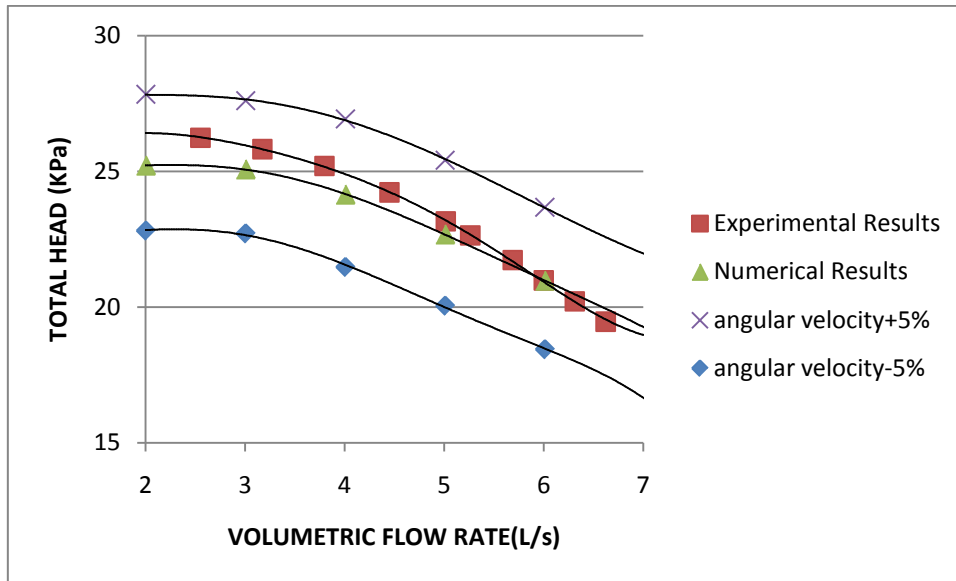
Figure 6.Total head through the pump.

At low flow rates, the differences between numerical and experimental results are larger while at higher flow rates the agreement is better, i.e, moving toward the design point. This better agreement close to the design point occurs due to the absence of complex secondary flows through the pump rotor which are very difficult to be captured by the numerical solution (suitable turbulence modelling for adverse pressure gradients and/or appropriate meshing refinement).

Besides, there are experimental uncertainties that affect the comparison. To check this effect, two additional simulations were undertaken with +/- 5% angular speed variations, Fig.6. It was verified that the numerical and experimental results for the total head are within the simulations with +/- 5% angular speed range.

Figure 7(a) presents the rotor cross plane normal to the pump rotating axis that splits the impeller-volute at medium section and the volute throat cross section, fig 7(b), which will be used for numerical results post-processing.
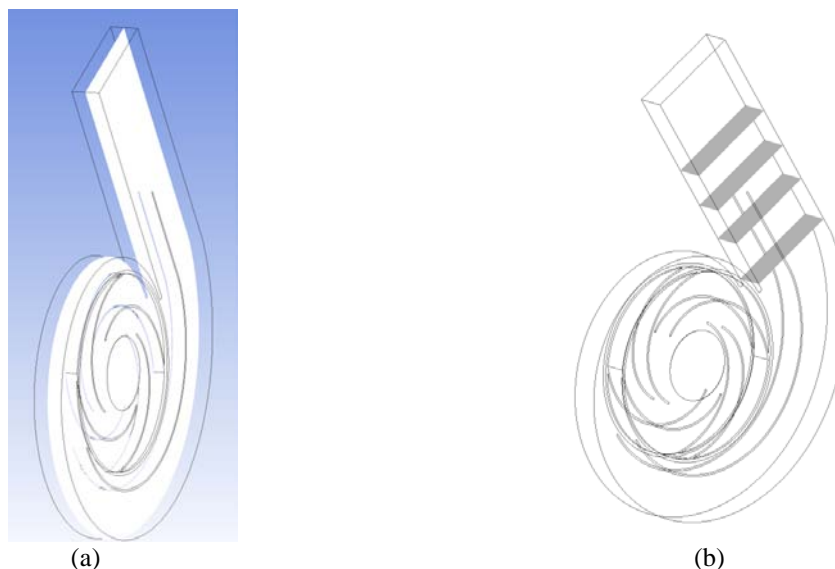

(a)   (b)

Figure 7. (a)Rotor cross plane normal to the pump rotating axis, (b) Volute throat cross section used to show numerical results.

It is verified that close to the design point, the flow describes more precisely the blade shape, Fig. 8(a). However, at off-design point, Fig. 8(b), it occurs non-tangential incidence flow, "shock regions", on the blades leading edge due to abrupt change in flow direction. Thus, for lower flow rate the passive resistances along the blade and changes of the channel section between the blades has a pronounced effect generating secondary flows at the impeller.
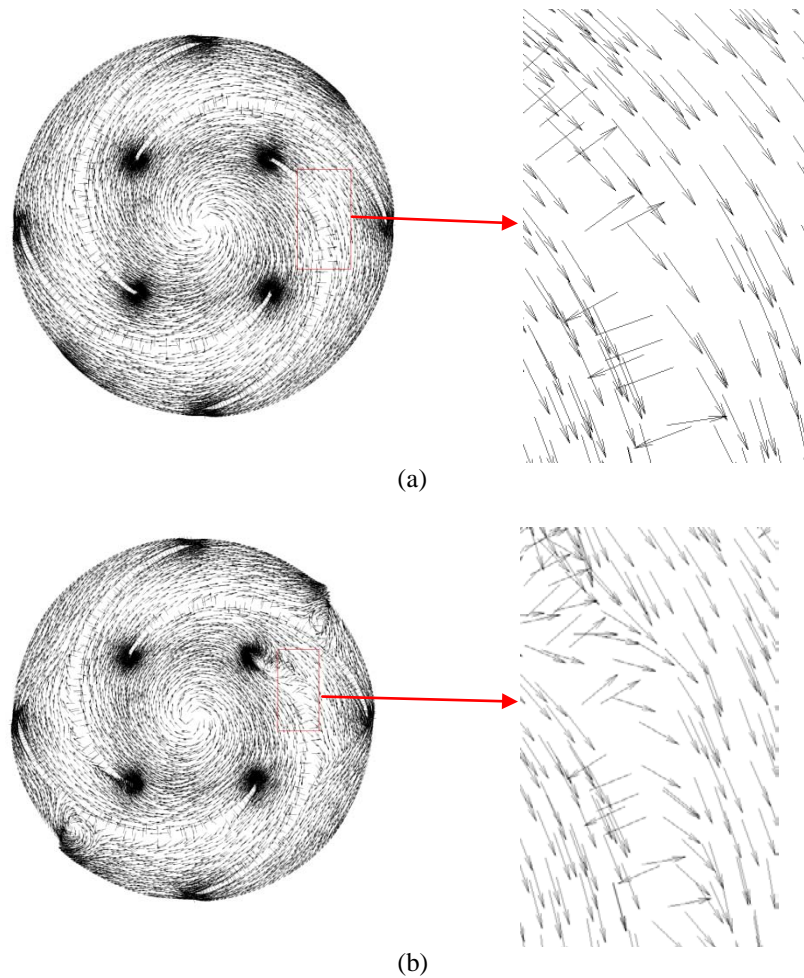
(a)

(b)

Figure 8. (a) Velocity vectors at design point pump capacity; (b) Velocity vectors at off-design pump capacity.

Figure 9 shows the tangential velocity vector at the rotor cross plane at off-design pump capacity operation. Due to large channel width and reduced blade number occurs an unsuitable rotor flow pattern which is characterized by non-uniform outlet velocity at rotor channel exit, Fig. 9(b).

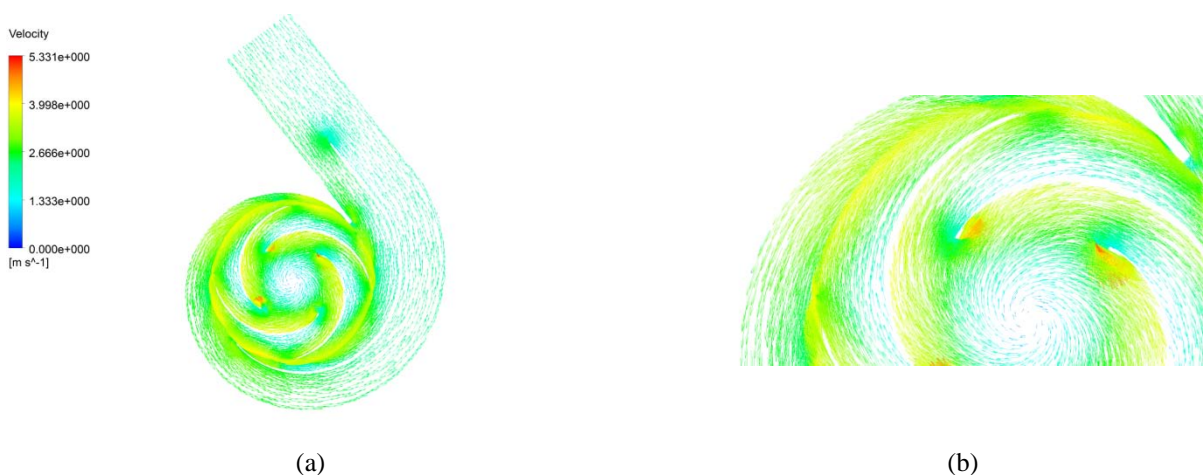(a)   (b)

Figure 9. (a) Tangential velocity vectors at the rotor cross plane; (b) Zoom close to the rotor outlet.

At the volute throat the velocity is essentially aligned with the walls, Fig10(a). At Figure 10(b) the velocity components are shown. The first component is normal to the cross section of the volute throat and the second tangential to the plane. Note that the tangential component has a minor magnitude therefore secondary flows are inexpressive at the exit of the volute. The kinetic energy grows up from the midstream to the walls at the impeller exit. An unstable shear flow is expected and consequently the mixture of the low energy and high energy streamline which represents loss.

Figure 10. (a) Velocity field at the cross section of volute throat; (b) Velocity components of the plane parallel to the volute outtake.

4. FINAL REMARKS

At the present work, the finite volume method is employed to solve the mathematical model of a centrifugal pump flow aiming to develop a validated methodology for Diesel engine cooling pumps design using CFD. The numerical results exhibit good agreement with experimental measurements for the total head.

The velocity field analysis allows indentifying efficiency loss factors, such as circulatory flow loss, detachment at the leading edge (shocks) and at the passage between the blades. Therefore, CFD tool allows obtaining pump flow variables at spatial-temporal domain with easier evaluation of pump´s efficiency degradation factors, which assists in the optimization of centrifugal pumps design.

5. ACKNOWLEDGMENTS

6. REFERENCES

Fluent Inc. Theory Guide, 12.0, February 2008.

Hamkins, C. P., Flack, R. D., 1987, "Laser velocimetry measurements in shrouded and unshrouded radial flow pump impellers" , American Society of Mechanical Engineering, vol 109, pp. 70-78.

Hangelstein, D., Hillewart, K., Van den Braembussche, R. A., Engeda, A., Keiper, R., Rautenberg, M., 2000,"Experimental and numerical investigation of the flow in a centrifugal compressor volute", American Society of Mechanical Engineering, vol 122, pp. 22-31.

Lucius, A., Brenner, G., 2010, "Unsteady CFD simulations of a pump in part load conditions using scale-adaptive simulation", International Journal of Heat and Fluid Flow, vol.31, pp 1113-1118.

Miner, S. M., Beaudoin, R. J., Flack, R. D., 1989, "Laser velocimetry measurements in a centrifugal flow pump", Journal of Turbomachinery, vol 111, pp. 205-212.

Ojeda, W., Flack, R. D., Miner, S. M., 1995, "Laser velocimetry measurements in a double volute centrifugal pump", Internationa Journal of rotating machinery, vol 1, pp. 199-214.

Ojeda, W., Flack, R. D., Miner, S. M., 1992, "Pressure distribution in a single and two version of a double volute of a centrifugal pump", ASME International Gas Turbine Conference, Paper 92-GT-20.

Spence, R., Amaral-Teixeira, J., 2009, "A CFD parametric study of geometrical variations on the pressure pulsations and performance charactheristics of a centrifugal pump", Journal of Computers & Fluids , Vol. 38, pp.1243-1257.

Uchida, N., Imaichi, K., Shirai, T., 1971, "Radial force on the impeller of a centrifugal pump", Bulletin of Japan Society of Mechanical Engineers, vol 14, pp 1106-1117.

Visser, F. C., Jonker, J.B., 1995, "Laser Doppler velocimetry flow measurements in the rotating frame inside the passage of a flow specific speed model centrifugal pump impeller", America Society of Mechanical Engineering FED, vol 229,pp. 145-157.

5. RESPONSIBILITY NOTICE